GEOPHYSICAL RESEARCH LETTERS, VOL. 26, NO. 14, PAGES 2097-2100, JULY 15, 1999

The March 25, 1998 Antarctic plate earthquake

Meredith Nettles, Terry C. Wallace and Susan L. Beck

Department of Geosciences, University of Arizona, Tucson

Abstract.
The March 25, 1998, Antarctic plate earthquake (M_W=8.1) occurred ~250 km from the nearest plate boundary, in oceanic lithosphere with an age of 35–55 my. Analysis of aftershock patterns shows that the earthquake ruptured a fault, or series of strike-slip fault segments, nearly 300 km long. The strike of the fault(s) is nearly perpendicular to the north–south trending fossil fracture zones which are the most marked bathymetric features of this region. Moment release during the mainshock was concentrated in two large subevents, clearly visible in the teleseismic body wave waveforms. Modeling of these body waves using a finite fault source places the first of the two subevents near the point of rupture initiation, on the eastern end of the fault, with the second large subevent occurring 220–280 km to the west. The two pulses of moment release are found to be separated in time by ~65 s. Comparison of the relative S wave amplitudes of the first and second pulses suggests that a rotation of the focal mechanism by ~10° occurred between the two subevents.

Introduction

The vast majority of earthquakes occur along the boundaries of the Earth's lithospheric plates, and reflect the relative motions across these plate boundaries. Intraplate earthquakes, however, occur in locations far removed from plate boundaries and manifest stresses and internal deformation within a plate. Intraplate seismicity is complex, and the tectonic driving mechanisms are poorly understood. Most often intraplate earthquakes occur on old zones of crustal weakness, such as rifts or sutures, that are reactivated by the present-day stress field, and some intraplate earthquakes may mark a rearrangement of plate boundaries.

On March 25, 1998, the largest oceanic intraplate earthquake (M_W=8.1) ever recorded occurred within the Antarctic plate (62.9°S, 149.5°E) north of George V Land, in an area for which there are no reports of previous seismicity. The seismic moment release of the earthquake was approximately four times as great as that of the next largest known oceanic intraplate earthquake (Nov. 30, 1983, Chagos Archipelago, Indian Ocean, M_W=7.7). The mainshock was followed by an energetic aftershock sequence which continues to this date. In the first 24 hours following the mainshock, 24 events with magnitudes (m_b) of 3.7 or greater were reported in the USGS Preliminary Determination of Epicenters (PDE). The preliminary International Data Centre (pIDC) located roughly twice as many similarly sized events during the same time interval.

The epicentral region of the March 25 earthquake is located approximately 300 km west of the Antarctic–Australian plate boundary (Figure 1). The plate boundary seismicity is dominated by left-lateral strike-slip earthquakes on transform faults connecting ridge segments (Figure 2). The best double-couple focal mechanism from the Harvard centroid–moment tensor (CMT) solution [*Dziewonski et al.*, 1999] for the mainshock is consistent with strike-slip motion on a north–south or an east–west plane; the sense of motion, however, is opposite to that of the transform fault seismicity (Figure 2).

In this paper, we investigate aftershock patterns and analyze body waves from the mainshock in order to determine the extent of faulting and the spatial and temporal history of slip during the March 25 earthquake. Such a characterization of the rupture process is a first step towards understanding the stresses which generated this unusual earthquake.

Analysis

We have relocated the 22 best recorded aftershocks of the Antarctic plate earthquake using a joint hypocentral determination (JHD) method [*Dewey*, 1983] (Figure 2). Despite the remote location of the earthquakes, at least 13 direct P wave arrival time measurements are available for each of the aftershocks we relocate, and typically ~25 direct P measurements are available for each event. Azimuthal coverage is quite good owing to the presence of stations in all of the southern hemisphere continents and the islands of the southwest Pacific. Initial hypocenters and phase data were taken from the PDE catalog; depths were held fixed in the inversion.

Two trends are apparent in the relocated aftershocks. The majority of the aftershocks lie along an east–west line, with the mainshock hypocenter near the eastern end of the zone of aftershocks. The length of the aftershock zone is ~300 km. No temporal development of the aftershock pattern is apparent from our analysis, but the CMT location places the center of moment release ~50 km to the west of the point of rupture initiation given by the travel times, within the zone of aftershocks, indicating rupture toward the west. The relatively good agreement between the rupture zone defined by the aftershocks and the east–west nodal plane of the double-couple portion of the CMT suggests that the mainshock occurred on an east–west trending fault, rather than on the north–south nodal plane as might be expected from

Paper number 1999GL900387.
0094-8276/99/1999GL900387$05.00

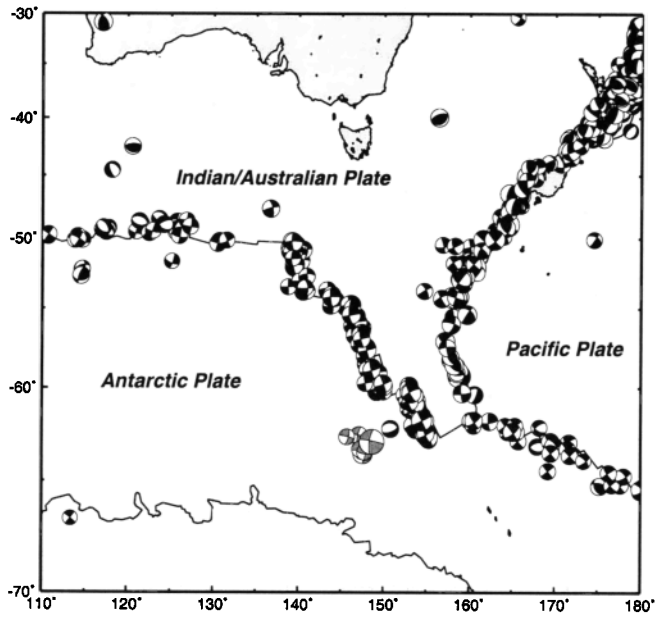

Figure 1. Map shows the location of the Antarctic plate earthquake sequence in its geographic and tectonic context. Focal mechanisms, shown in equal-area lower-hemisphere projection, are from the Harvard CMT catalog (best double-couple only), with earthquakes occurring 1976–March 1998 shown in dark grey and the earthquakes of the Antarctic plate sequence shown in light grey. Plate boundaries from the compilation of *Müller et al.* [1997] are also shown.

the alignment of the fossil fracture zones in the area. The pattern of aftershocks agrees well with that found by *Wiens and Wysession* [1998].

A second trend in the aftershock locations, with a length of ~100 km, runs from the center of the primary trend toward the south. The locations of the two largest aftershocks fall within this secondary trend, with the largest aftershock lying at its southern end. The orientation of the north–south trending aftershocks is in good agreement with the orientation of the N–S nodal plane of the largest aftershock; it is therefore possible that the largest aftershock, despite having a focal mechanism very similar to the double-couple part of the mainshock focal mechanism, occurred on a conjugate fault nearly perpendicular to that of the mainshock. Similar aftershock patterns were observed for the 1987–88 Gulf of Alaska earthquakes [*Hwang and Kanamori*, 1992; *Pegler and Das*, 1996] and for the 1992 Landers earthquake [*King et al.*, 1994], and aftershocks of large magnitude occurred on the conjugate faults in each of these cases. We note, however, that the aftershock locations within this secondary trend are also consistent with interpretation in terms of a series of E–W trending faults parallel to that on which the mainshock occurred.

We constrain the spatial and temporal development of the mainshock rupture by analysis of the teleseismically recorded body wave waveforms. The P waveforms are complex and of long duration, and few SH records without interfering phases (ScS) are available. Large, well-separated arrivals corresponding to at least two distinct episodes of moment release during the earthquake are evident in the waveforms, however, and these arrivals make it possible to resolve the relative locations and timing of the largest subevents which comprise the mainshock. We model the broadband P and S displacement waveforms using the wavelet stripping method of *Kikuchi and Kanamori* [1991]. We attempt the inversion using two different focal mechanisms, which remain fixed during the inversion: the first has nodal plane orientations determined from the best-fit line through the relocated aftershocks, with an assumption of pure strike-slip motion on a vertical fault plane; the second mechanism corresponds to the double-couple portion of the CMT solution for the mainshock (Figure 2). While the CMT solution does have a large non-double-couple (NDC) component, the double-couple part of the solution agrees well with the CMT solutions for the aftershocks; in addition, we find that the key elements of the seismograms can be reproduced without introducing an NDC component into the focal mechanism.

We perform the body wave inversion using both the east–west and the north–south nodal planes as the fault plane and require subevents of the earthquake to lie in this plane. For both focal mechanisms, synthetic seismograms calculated using the east–west plane contain the most significant features of the observed waveforms (Figure 3), in particular, the two large amplitude arrivals separated by ~65 s. The largest episode of moment release during the mainshock is found to have occurred on the eastern portion of the fault, with the second large subevent occurring 220–280 km to the

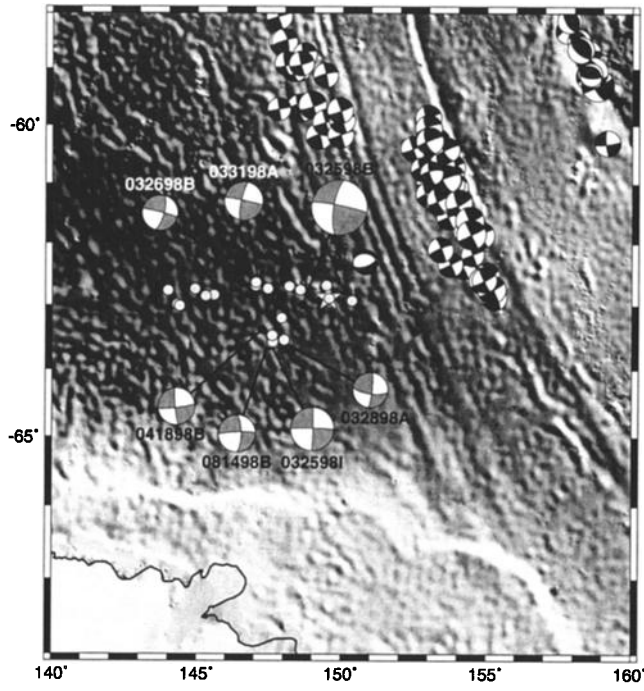

Figure 2. Aftershock locations determined in this study (light dots) and CMT solutions are shown with two minute bathymetry [*Smith and Sandwell*, 1997], illuminated from the northeast. Star shows location of the mainshock hypocenter as determined by NEIS. CMTs for earthquakes of the intraplate sequence are shown with their Harvard event file names; we note that the full moment tensor solution for the mainshock contains a large non-double-couple component, which is not shown here.

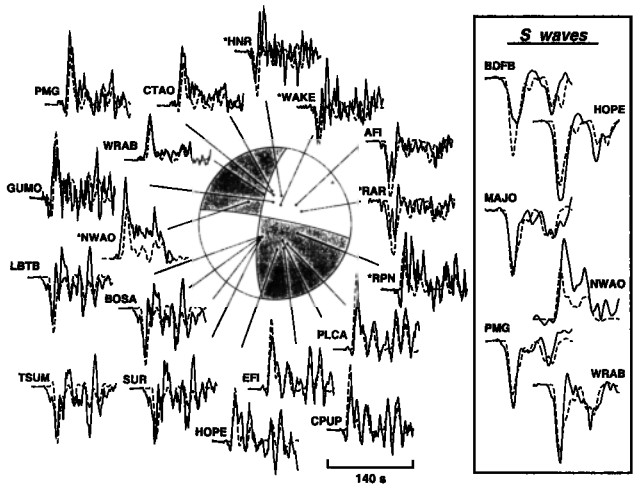

Figure 3. Results from joint P and S waveform inversion using a focal mechanism based on the Harvard CMT solution, fixed at 15 km depth. Observed seismograms are shown as solid black lines; synthetic seismograms are shown as dashed lines. A * indicates traces not included in the inversion due to higher noise levels near the first arrival or potential interference from phases not modeled.

west (Figure 4). Results from independent inversions of the P and S waveforms are consistent with the extent of rupture determined from the aftershock distribution, as are the results from a joint inversion of the P and S waves, shown in Figures 3 and 4. We prefer the results obtained using the CMT focal mechanism to those achieved using the alternate mechanism, but find that the waveforms are better fit when the source is placed at a depth of ~15 km, as compared with the 29 km reported in the CMT catalog [*Dziewonski et al.*, 1999].

Rupture on a north–south trending fault does not explain the data well. Waveforms from stations to the south of the earthquake are particularly poorly fit by synthetic seismograms generated for a north–south striking fault plane: the inversion is unable to find a location for the second major pulse of moment release which agrees consistently with the timing of the large arrivals in the latter part of the seismograms. In addition, the seismic stations PMG and HOPE lie almost directly north and south of the epicenter, respectively, and the SH waveforms from the Antarctic event were well recorded at these two stations, giving us very good control on the best placement of subevents on a hypothetical north–south fault plane. The arrival times of the second pulse relative to those of the first pulse are very nearly identical at PMG and HOPE, suggesting that the source of the second pulse is displaced neither north nor south of that for the first pulse. In contrast, stations to the east and west exhibit relative arrival times which vary by as much as 10 s, with stations to the west having shorter intervals between the two pulses.

A change in the geometry of faulting between the first and second large subevents is suggested by the rather dramatic differences in the character of SH waveforms recorded at four stations in southern Africa (SUR, TSUM, BOSA and LBTB; see Figure 5). The displacement due to the second pulse of moment release described above is small enough to make identification difficult at SUR and TSUM, whereas this pulse is clearly visible at BOSA and LBTB, located only a few hundred km to the east. The stations are located quite close to a node in the S wave radiation pattern, and the observed change in the amplitude ratio of the first pulse to the second is consistent with a slight rotation in the fault plane between the first and second subevents. We plot observed amplitude ratios for the 18 stations for which SH waveform data are available versus that predicted for a rotation of the fault plane from 281° to 271° in Figure 5. For no rotation, the amplitude ratio should be constant across all azimuths from the source; we find good agreement between our observations and a rotation of 10±5° in the orientation of the fault plane. Rotation of the fault plane implies either a curved, single fault or two fault segments of slightly different orientations. This curvature in the fault, along with the heterogeneous slip distribution we observe, is similar to that seen for the Landers earthquake [*King et al.*, 1994] and raises the possibility that, as at Landers, some aftershocks may be the result of stress triggering on nearby faults.

Discussion

The large size of the Antarctic plate earthquake can be taken as an indication of the buildup of high stress levels within the plate. We estimate the static stress drop in the earthquake to be ~190 bars, using the scalar moment deter-

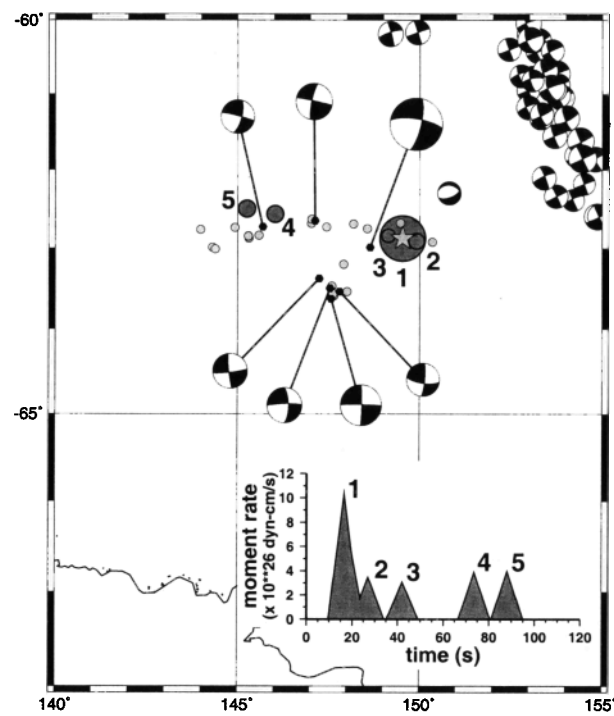

Figure 4. Map shows the locations of the subevents (darker circles) found by joint inversion of P and S waveforms, using the focal mechanism shown in Figure 3. Size of circles is proportional to moment release; timing of subevents is shown at lower right. The total moment release represented by the subevents shown here is 1.75×10^{28}dyn-cm, similar to the moment obtained in the CMT analysis. Aftershock locations and CMT solutions are shown for reference.

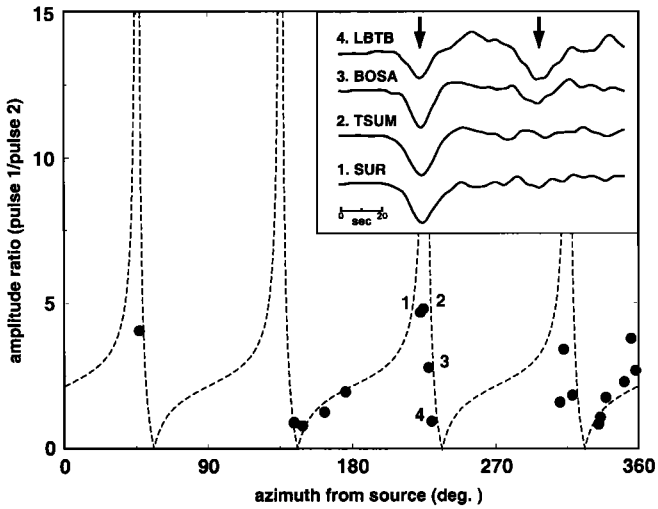

Figure 5. Displacement amplitude ratios for the first large pulse of moment release with respect to the second, measured (black dots) from the available SH waveforms and predicted (dashed line) based on S wave radiation patterns for the case in which the fault plane of the second subevent is rotated 10° from that of the first subevent; for no rotation, a constant value would be expected. SH waveforms from four African stations, described in the text, are shown at upper right. A marked decrease in the relative amplitude of the second pulse evident in the seismograms occurs as the azimuth from the source changes across the stations from SUR to LBTB.

mined from the Harvard CMT (1.7×10^{28}dyn-cm), a fault length of 250 km, and a total fault width of 15 km. This high value is also suggestive of a large stress buildup within the plate, but we note that this result is highly dependent on the assumed width of faulting, and that a deeper average extent of faulting greatly reduces the calculated stress drop. The ocean floor has an age of 35–55 my [*Müller et al.*, 1997] in the aftershock zone, which corresponds to a lithospheric thickness of ~50–90 km, and a seismogenic zone (500° isotherm) of ~10–16 km. The CMT analysis, however, places the centroid depth for the earthquake at 29 km.

It is difficult to explain the Antarctic earthquake in terms of tectonic driving stresses for this region as we currently understand them. The epicenter of the earthquake is located more than 250 km from the nearest plate boundary; it lies ~600 km southwest of the junction of the Antarctic, Pacific and Australian plates (the Macquarie triple junction). None of the usual explanations for oceanic intraplate earthquakes — thermal stressing of the lithosphere, effects of differential topography, stresses associated with volcanic activity, or deformation associated with a diffuse plate boundary [*Wiens and Stein*, 1983], for example — appear to apply in this case.

It is possible that the Antarctic earthquake is a result of plate boundary rearrangement occurring near the tectonically complex Macquarie triple junction. A change in the pole of rotation, such as that observed for motion between the Pacific and Antarctic plates [*Stock and Molnar*, 1982], often leads to a situation in which the geometry of plate boundaries is no longer consistent with relative plate motions. Strain which is not accomodated on the boundaries is then transmitted into the interior of the plates. Such a change, and the resulting inability of the ridge-connecting transform faults to accomodate all of the relative motion across the plate boundary, might then explain our observation that failure in this case occurred nearly perpendicularly to the fracture zones. Though the fracture zones are presumably weaker than the surrounding oceanic crust, they maintain the trend of the transform faults they once were.

Acknowledgments. The authors wish to acknowledge helpful discussions with D. Dreger, G. Ekström, R. Stein and D. Wiens. This work was supported by NSF grant EAR-97-06219 . SASO contribution #111.

References

Dewey, J. W., Relocation of instrumentally recorded pre-1974 earthquakes in the South Carolina region, *in* Studies related to the Charleston, South Carolina earthquake of 1886, G. S. Goh, ed., USGS Prof. Paper 1313, Q1-Q9, 1983.

Dziewonski, A. M., G. Ekström and N. N. Maternovskaya, Centroid-moment tensor solutions for January-March 1998, Phys. Earth Planet. Inter., *in press*, 1999.

Hwang, L. J. and H. Kanamori, Rupture processes of the 1987–1988 Gulf of Alaska earthquake sequence, *J. Geophys. Res.*, *97*, 19881–19908, 1992.

Kikuchi, M. and H. Kanamori, Inversion of complex body waves—III, *Bull. Seismol. Soc. Am.*, *81*, 2335–2350, 1991.

King, G. C. P., R. S. Stein and J. Lin, Static stress changes and the triggering of earthquakes, *Bull. Seismol. Soc. Am.*, *84*, 935–953, 1994.

Müller, R. D., W. R. Roest, J.-Y. Royer, L. M. Gahagan and J. G. Sclater, Digital isochrons of the world's ocean floor, *J. Geophys. Res.*, *102*, 3211–3214, 1997.

Pegler, G. and S. Das, The 1987–1992 Gulf of Alaska earthquakes, *Tectonophysics*, *257*, 111–136, 1996.

Smith, W. H. F. and D. T. Sandwell, Global sea floor topography from satellite altimetry and ship depth soundings, *Science*, *277*, 1956–1962, 1997.

Stock, J. and P. Molnar, Uncertainties in the relative positions of the Australia, Antarctica, Lord Howe, and Pacific Plates since the late Cretaceous, *J. Geophys. Res.*, *87*, 4697–4714, 1982.

Wiens, D. A. and S. Stein, Age dependence of oceanic intraplate seismicity and implications for lithospheric evolution, *J. Geophys. Res.*, *88*, 5455–6468, 1983.

Wiens, D. A. and M. E. Wysession, Recent oceanic intraplate earthquake in Balleny Sea was largest ever detected, *Eos Trans. AGU*, *79*, 353–354, 1998.

S. L. Beck, M. Nettles, T. C. Wallace, Department of Geosciences, Building #77, University of Arizona, Tucson, AZ 85721. (e-mail: beck@geo.arizona.edu, nettles@geo.arizona.edu, wallace@geo.arizona.edu)

(Received September 30, 1998; revised March 8, 1999; accepted March 23, 1999.)